STYRELSEN FÖR VINTERSJÖFARTSFORSKNING
Sjöfartsverket Sverige, Sjöfartsstyrelsen Finland
Forskningsrapport nr 16:7

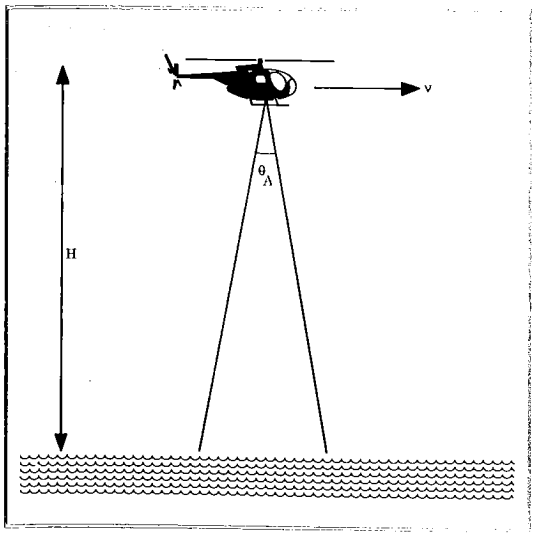

Radar altimeter results

by Sune Axelsson
Linköping 1976

WINTER NAVIGATION RESEARCH BOARD
Swedish Administration of Shipping and Navigation, Finnish Board of Navigation
Research Report No 16:7

SEA ICE 75
Radar altimeter results

by Sune Axelsson
SAAB-SCANIA AB
Missile and Electronics Sector
Linköping 1976

Table of Contents

Foreword 4

Preface 5

Abstract 6

1. Introduction 7

2. Theoretical Background 8
2.1 Introduction 8
2.2 Application to Sea-Ice 9
2.3 Attenuation of Sea-Ice 11

3. Summary of the Programme 12
3.1 Parameters to be Measured 12
3.2 Ground Truth Areas 12
3.3 Flight Programme 13

4. Instrumentation 14
4.1 Radar Altimeter 14
4.2 Recording System 14
4.3 Data Analysis 15

5. Experimental Results 16
5.1 Passages Over Ice-Ridges 16
5.2 Influence of Snow and Water 17
5.3 Runs Over Thin Ice 18
5.4 Ice/Water Passages 18
5.5 Recordings from the 1x1 km Area 20
5.6 Spectral Characteristics 23

6. Conclusions and Recommendations 25

References 27

Foreword

The Winter Navigation Research Board presents report No. 16:7. One of the instruments used during the remote sensing experiment SEA ICE-75 was a radar altimeter developed by Saab-Scania AB. In this report Sune Axelsson describes the instrument and the results obtained from the test flight.

The Winter Navigation Research Board would like to take the opportunity to thank the author of this report as well as others engaged in different phases of the experiment. Thanks are also extended to the Swedish Board for Space Activities for enabling the Swedish Space Corporation to engage Saab-Scania in the project.

Norrköping and Helsinki, July 1976.

Lennart Johansson **Helge Jääsalo**

Preface

This report describes the results obtained at a field test on sea-ice mapping by radar altimetry. The experiment was carried out in the Gulf of Bothnia, March 1975. At the same time period, other types of airborne sensors were also tested. The whole experiment was coordinated by the Swedish Meteorological Institute, the Swedish Research Institute of National Defense, and the Swedish Space Corporation.

The participation of Saab-Scania was financed by the Swedish Space Corporation. A helicopter was placed to the disposal of Saab-Scania during the test period by the ice-breaking Service of the Swedish Administration of Shipping and Navigation.

Several persons at Saab-Scania were engaged in different phases of the experiment. Göran Ohlsson and Tommy Bergström were responsible for the installation on the helicopter. Håkan Lövsén made the necessary modifications of the altimeter prototype and operated the equipment during the flight programme. The support from Kasselflyg AB in the installation phase and from the crew of the ice-breaker TOR during the test period is also gratefully acknowledged.

Abstract

The present paper describes the results obtained at a field experiment with radar altimetry above sea-ice, carried out in the Gulf of Bothnia, March 1975. The results of the experiment indicate that the envelope detected noise of the altimetry output signal can be used for measurements on ice ridges and other large-scale surface roughnesses. The spectral characteristics of the signal also give some information about the surface roughness. The AGC-signal, which is a measure of the reflectivity of the ground surface, may be used to distinguish ice from water as well as snow-covered ice from non-covered ice. As the weather was mild during the whole test period further measurements should be carried out during a period of cold weather. Some modifications of the altimetry equipment are also recommended.

1. Introduction

The economic development of industries in Norrland is much depending on whether the shipping lanes can be kept open the whole year. A necessary condition for shipping even in winter is that sufficient information on the sea-ice situation is available to the Ice-breaking Service for immediate operational purposes, and to the Swedish Meteorological and Hydrological Institute (SMHI) for forecasting of the ice situation the next days. The forecasts give the required information for shipping in choosing the most economic routes.

As very large ice-areas are to be mapped in a short time, remote sensing from airborne or spaceborne platforms seems to be a well- adapted technique for sea-ice mapping. In order to evaluate the capability and possible limitations of different types of remote sensing methods, a field experiment was organized in the Gulf of Bothnia in March 1975. The experiment was carried out in cooperation between different institutions in both Finland, the Netherlands and Sweden. Multi-band photography, IR- and microwave radiometry as well as different types of radar methods were tested at the experiment. A detailed description of the general programme can be found in [1].

In this report, the results of the radar altimetry experiment are desribed. A detailed programme for the tests with this equipment is given in [2].

2. Theoretical Background

2.1 Introduction

When a radar altimeter of FMCW-type is used above a rough sea-ice surface, the reflected signal becomes very complex to describe and analyse due to the fact that signals are received from both different directions and different ranges. An analytical model for radar altimetry above a rough surface was studied in detail in [3] — [4]. The model can be used to describe the altitude output in statistical terms, if the following conditions are fulfilled:

a) Signals from a great number of reflectors are received by the altimeter

b) No reflector yields a return signal, which is large compared with the sum of all the others

c) The phase angles of the reflected signals are uniformly distributed over 2π

d) The phase angles of signals received from different reflectors are statistically independent

If the received power versus the distances to the reflectors is given by p(R), the unsmoothed altitude output (H_m) can be desribed by

$$H_m = \tilde{R} + \xi \tag{2.1}$$

where $\tilde{R}$ is the weighted average distance to the different reflectors i.e.

$$\tilde{R} = \int_0^\infty R\, p(R)\, dR \tag{2.2}$$

For amplitude and frequency measuring FMCW-radar altimeters, the probability density function of the unsmoothed altitude noise ξ is given by [3] — [4]

$$p_1(\xi) = \frac{1}{2} \frac{\sigma_r^2}{\left[\xi^2 + \sigma_r^2\right]^{3/2}} \tag{2.3}$$

where

$$\sigma_r^2 = \int_0^\infty (R - \tilde{R})^2 p(R)\, dR \tag{2.4}$$

As can be shown from Eq. (2.3), the mean deviation of the altitude noise from its mean value is

$$m = \int_{-\infty}^{\infty} |\xi|\, p_1(\xi)\, d\xi = \sigma_r \tag{2.5}$$

The noise signal $\xi(t)$ varies much more rapidly with time than $\tilde{R}(t)$, which follows the local mean value of the surface profile.

A rough estimation of the bandwidth of the altitude noise is given by the doppler bandwidth

$$B_d = \frac{2v}{\lambda} \theta_A \tag{2.6}$$

where

v = the velocity of the platform

λ = the electromagnetic wavelength of the carrier wave

θ_A = the lobe width of the sensitivity lobe (in radians)

A vertically directed sensitivity lobe and a horizontal velocity vector are also assumed (Figure 2.1).

Example: For $\lambda = 0{,}07$ m, $\theta_A = 0.5$ rad, $v = 15$ m/s (30 knots), $B_d = 215$ Hz is obtained.

This value should be compared with the bandwidth of the profile signal (f_p), which is of the order $v/2\pi\theta_A H$ with H = altitude. For $H = 4$ m, the cut-off frequency of the profile signal is only about 1 Hz.

Due to the great differences in spectral distribution between the altitude noise and the slow altitude fluctuations caused by the surface profile, these two components can easily be separated by passing the altitude output signal through two band-pass filters with non-overlapping pass-bands. The lower pass-band separates the profile information and the higher one extracts the altitude noise component.

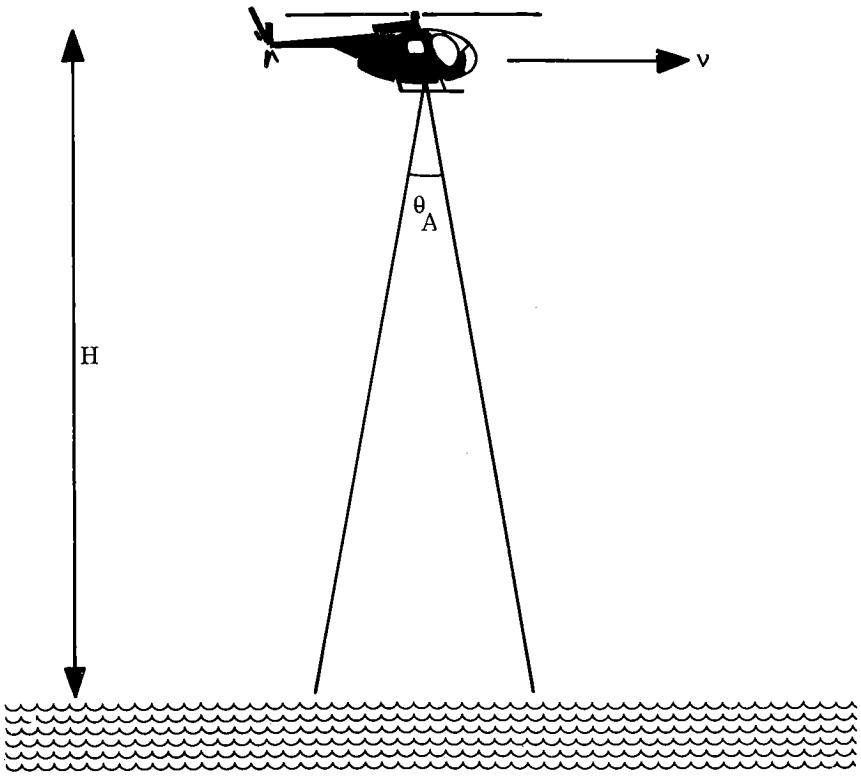

Figure 2.1: *Definition of the geometry.*

2.2 Application to sea-ice

A relevant question now is: How representative is the analytical model for sea-ice measurements? Contrary to ice on lakes or close to the shore, the sea-ice has usually a rather rough surface structure. Due to the wind stress, folded ice-layers and ice ridges, composed by ice-floes with different orientations, occur frequently. These ridges are often much higher than the surrounding ice and the thickness of the individual ice-floes. When the altimeter passes an ice-ridge, reflected energy is thus obtained simultaneously from different surface elements within the lobe — from the lower part of the ridge and the surrounding ice to the top of the ridge. As the height of a ridge is many wavelengths, the preconditions of the model can be considered approximately satisfied.

It is obvious from Eqs. (2.4) and (2.5) that the height of the ridge will influence the noise level of the altitude output. The detailed distribution of power versus range has also an effect, however. Figure 2.2 shows some examples.

Case A of Figure 2.2 represents the case, when reflections are primarily obtained from only two distances, e.g. the upper and lower boundaries of sea-ice. The maximum altitude noise occurs, when the same amount of reflected power is generated from the two boundaries. In that case, $\sigma_r \mathrm{Max} = 0.5$ d is obtained where d is the ice thickness. If the received

power from one boundary is reduced to 10%, the mean deviation of the altitude noise is reduced to 0.3 d.

In case B, the reflected power is uniformly distributed between two ranges giving $\sigma_r = d/\sqrt{12} \approx 0.29$ d.

A triangular distribution according to case C reduces the altitude noise to $\sigma_r \approx 0.24$ d. In case D, a further reduction is obtained $\sigma_r \approx 0.20$ d.

Case B—D are probably the most representative distributions for ice ridges. An estimate of the height of the ridges $\hat{h} = 4\sigma_r$, yields an error less than 20% in that case.

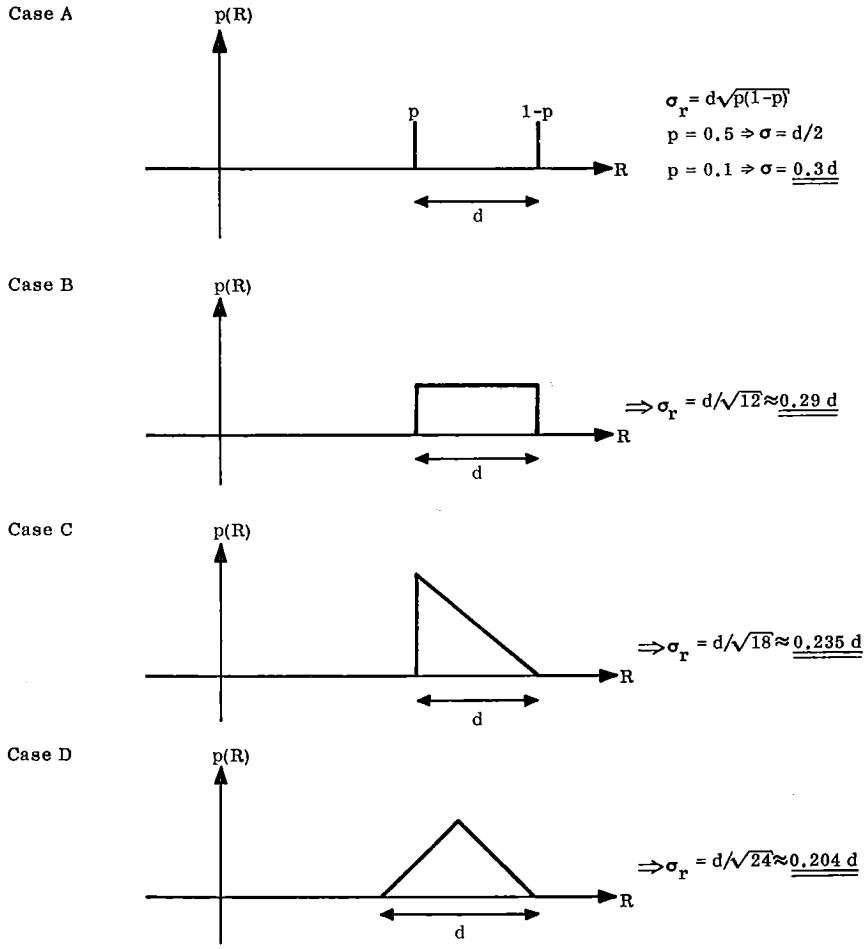

Figure 2.2: *The range spread parameter σ_r for different forms of the range scattering function.*

Concluding, the analytical model discussed in [3]—[4] can be applied to sea-ice in case of rough ice and ice-ridges. For ice thickness measurements, the surface boundaries must be sufficiently rough, if the conditions a)—d) are to be fulfilled. The sea-ice must also be semi-transparent so that at least 10% of the received power originates from the ice-water boundary. A reasonable estimate of the ice thickness is then $\hat{d} \approx 3\sigma_r$.

A critical point may be the number of reflectors N, which are simultaneously within the antenna lobe at the extremely low altitudes of the test flights. The consequences of only two reflectors within the lobe were analysed in detail in a separate report [7]. The results show that a two-reflector model and a multi-reflector model give deviating results both at the description of bias and distribution of the altitude noise. The difference in mean deviation of the altitude noise, predicted by the two models, is not too great, however. The error introduced for $N = 2$ is of the same order as the error introduced by a changed distribution of the power

Due to the unsymmetric distribution of the altitude noise in the two-reflector case, this case can be identified by studying the recordings of the altitude noise [7]. At the analysis of the noise signals obtained at the experiment, no significant unsymmetry of the altitude noise was detected.

Therefore, the multireflector model seems to be an appropriate description of the reflected signal from a rough sea-ice surface.

Figure 2.3: *Photo of a typical ice ridge.*

2.3 Attenuation of sea-ice

As pointed out in [6], the transmission properties of sea-ice is much depending upon the ice temperature. The attenuation constant and penetration depth versus ice temperature are shown in Figure 2.4 The day-time air-temperature during the whole test period varied between —6°C and +3°C. Therefore, a penetration depth less than 0,1 m can be expected at f=5 GHz during the period, which also means that signals from the underside of the ice were highly suppressed for ice-thicknesses greater than 0,2 m. This fact was also justified by the microwave radiometry measurements [8], which were carried out at two different frequency bands, 600 MHz and 4.7 GHz. Very weak signal fluctuations were obtained in the 4.7 GHz channels, while significant signal variations were generated at 600 MHz. At earlier Finnish microwave radiometry measurements in the winter 73/74, which were carried out at lower air temperatures, the recordings at 600 MHz and 4.7 GHz were very similar [9].

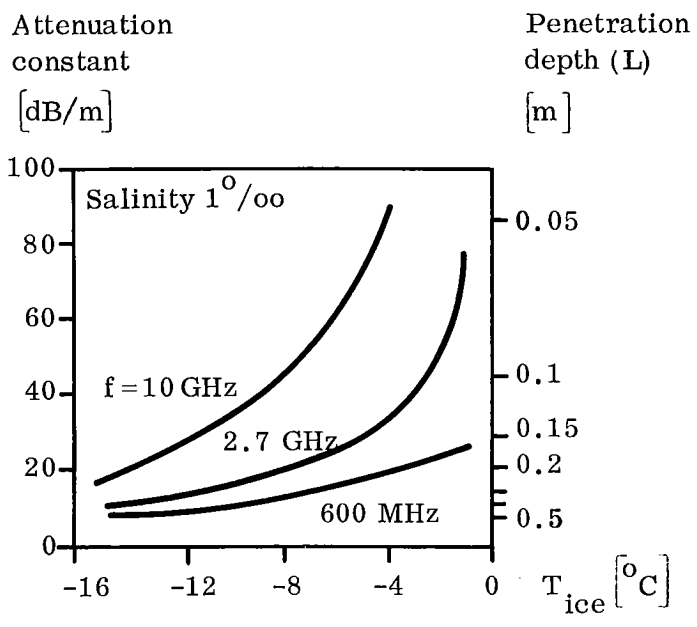

Figure 2.4: *Attenuation constant and penetration depth versus ice temperature for sea ice. According to [6].*

As a result of the low penetration depth in ice at high air temperatures, it is reasonable to assume that the variations in noise level during the test period were mainly generated by large-scale surface roughnesses and to a minor extent by variations in the ice thickness itself.

3. Summary of the Programme

3.1 Parameters to be measured

Several parameters influence the remote sensing signature of the sea-ice. The following parameters are the most important onnes for the user [1]:

- ☐ ice or non-ice
- ☐ ice concentration
- ☐ roughness of the ice
- ☐ ice-thickness
- ☐ state of ice surface (melting ice, snow-covered ice etc.)
- ☐ type of ice

Detailed information on these ice parameters within a limited area will make it possible to choose the optimum route during the next 6—10 hours. If large-scale information on the ice-parameters is available for the whole sea area, the development and movements of the sea-ice can be forecasted for the next 1—10 days [1].

Often the recorded remote sensing signals are also influenced by environmental parameters — like temperature (of ice, water and air), wind speed, which makes the interpretation more difficult. It is, therefore, also of interest to study how these parameters influence the output signals of the sensors.

3.2 Ground truth areas

The ice measurements were carried out over ground truth areas of different sizes 1x1 km, 5x5 km and 15x15 km, respectively [1]. The altimetry measurements were concentrated to the 1x1 km area, which is shown in Figure 3.1. The ice thickness in this area was measured every 200 m and

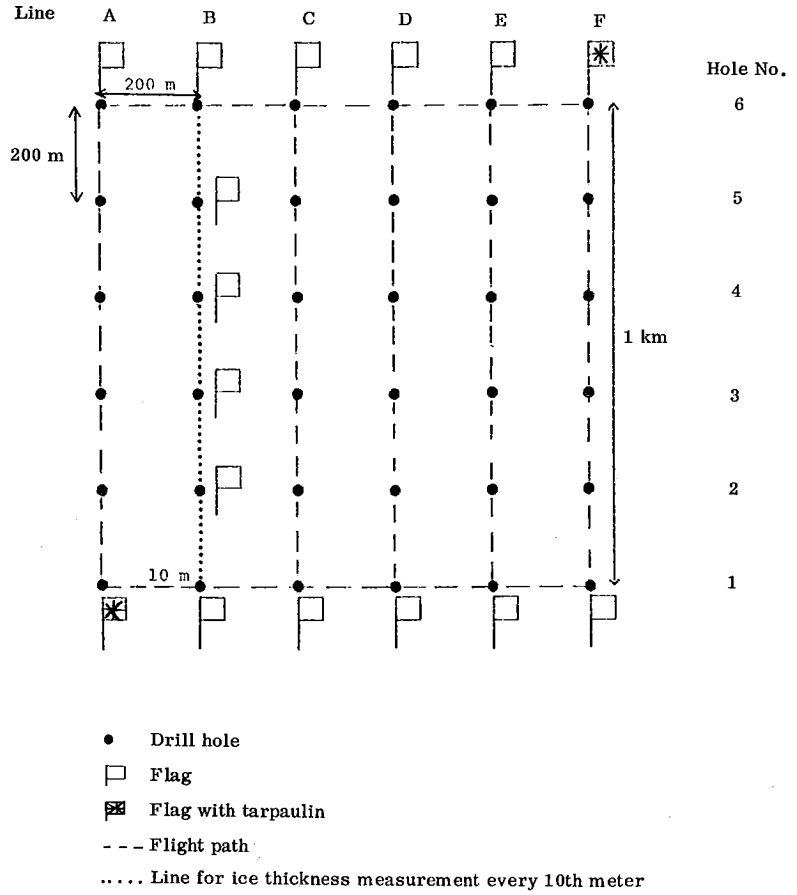

Figure 3.1: *Ground truth area 1x1 km.*

along line B every 10 m. Existing ice ridges and ice roughnesses were also mapped. Snow thickness, temperature data, cloudiness, wind speed etc. were measured by SMHI, which was responsible for the collection of ground truth data.

3.3 Flight programme

The radar altimeter was mainly tested above the 1x1 km area. Repeated runs were also made over an area with high ridges and over ice/water boundaries.

In order to test the influence of snow and water on the remote signals, the snow was removed from a rectangular part of the ice. About half the area was flooded with water.

Most runs were carried out at an altitude of 4 m and a speed of 30 knots. In some cases, recordings were also obtained from 10 m and 60 knots. Along the transportation route Luleå-TOR, recordings were obtained over various types of ice from different altitudes. However, there were no accurate ground truth data available, in that case, which makes a detailed interpretation difficult.

4. Instrumentation

4.1 Radar altimeter

The sensor used at the experiment was a C-band radar altimeter of FMCW type, developed at the Avionics Development Department of Saab-Scania. The radar altimeter was carried by a helicopter of type LAMA 315 B, under which the altimeter was mounted in a cylindrical pod. The two antennas of the altimeter are down-looking with a beam-width of about 30 degrees. The pod was connected to a power unit and a tape recorder, both placed inside the helicopter.

4.2 Recording system

Three output signals from the radar altimeter were recorded simultaneously on a four-channels tape recorder (Tandberg Instrumentation Recorder Series 115). The fourth channel was used by the operator in order to memorize all types of information which is necessary for the interpretation of the recorded data, such as time, altitude, speed, type of ice, times of passage over ridges, ice/water boundaries etc.

The following three output signals were recorded

- ☐ altitude signal H(t)
- ☐ altitude fluctuations h(t)
- ☐ AGC-signal

The altitude fluctuations, which contain the profile information and the altitude noise generated by the altimeter, were outfiltered in a separate channel in order to suppress the noise contribution from the tape recorder.

The AGC-signal increases with increasing level of the received signal and is therefore a measure of the reflectivity of the surface below the altimeter.

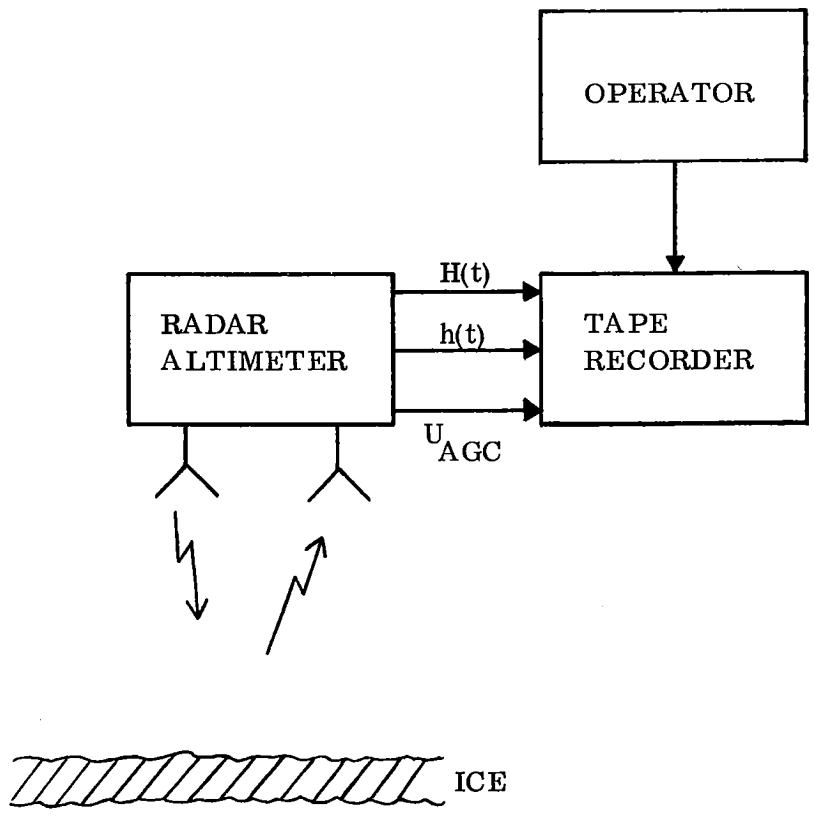

Figure 4.1: *A simplified block-diagram of the recording system.*

4.3 Data analysis

The raw-signals, recorded on the tape-recorder must be further processed before the interpretation, if the useful information is to be extracted. For the analysis of the recorded signals, an experimental equipment according to Figure 4.2 was used.

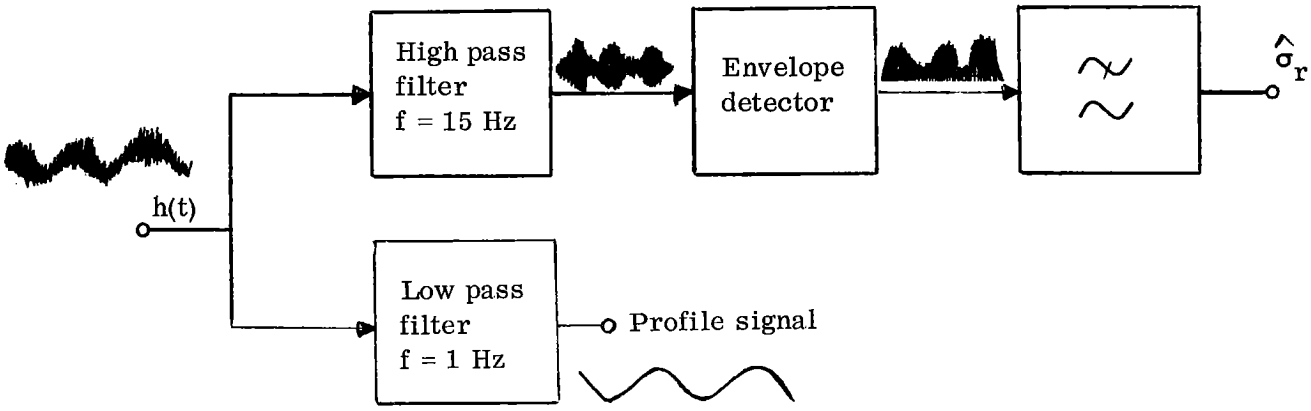

Figure 4.2: *Signal processing at the analysis of the raw-data.*

The output signal h(t), representing the fluctuations of the altitude signal, is connected to a high-pass filter and a low-pass filter so that the profile signal and the more rapidly varying noise component can be separated into two parallel channels. The mean deviation of the noise component is then estimated by passing the high-pass filtered signal through an envelope detector. At the analysis, the time constant of the envelope detector was varied, as well as the cut-off frequency of the high-pass filter.

The preliminary tests of the recorded data showed that the most significant information was obtained from the high-pass filtered noise signal. The low-frequency profile signal did not indicate ridges as well. As the low-frequency altitude variations of the helicopter may also introduce an error, when the profile signal is used, only the recordings of the estimated altitude noise and the AGC-signal are discussed in the next chapter.

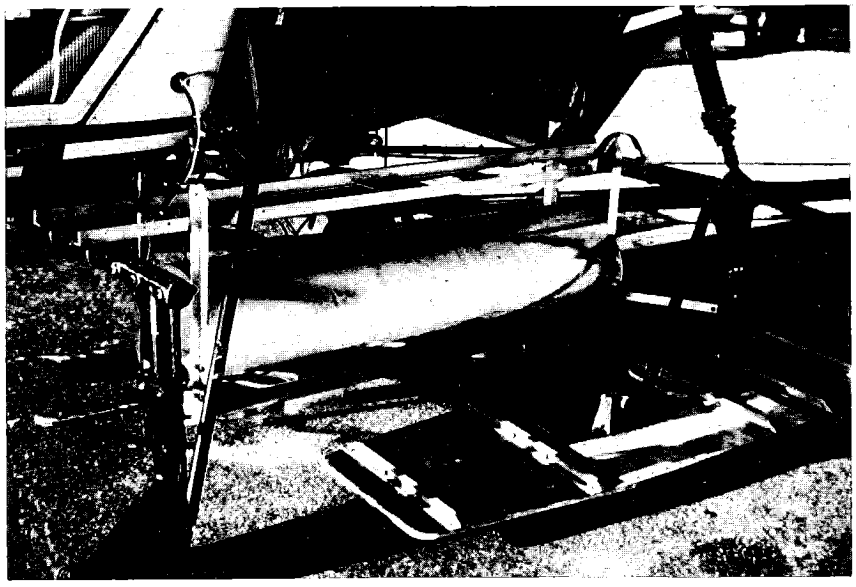

Figure 4.3: *The installation of the altimeter pod on the helicopter.*

5. Experimental Results

5.1 Passages over ice-ridges

Two repeated runs were made over an area with high ice-ridges. The largest ridges had a height of 1,9 m. The AGC-signal and the mean deviation of the altitude noise are shown in Figures 5.1—5.2. The comments of the operator during the run are also shown.

The recordings show that the individual ridges can be identified by the highly increased altitude noise. Folded ice gives a lower and more

Figure 5.1: *Altitude noise (mean deviation) and AGC-signal at the first run over an area with high ice-ridges. Increasing U_{AGC} is equivalent to increasing reflectivity of the ground surface. Altitude: 4 m. Velocity 30 knots.*

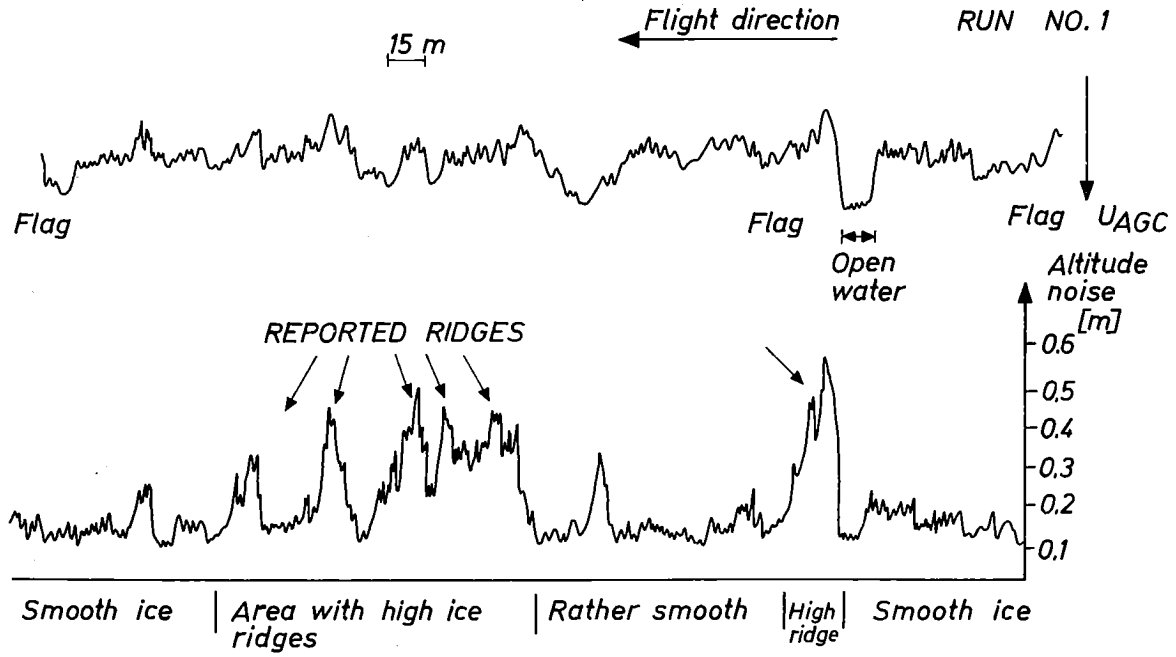

Figure 5.2: *Altitude noise and AGC-signal at the second run over the area with high ridges. Altitude: 4 m. Velocity: 30 knots.*

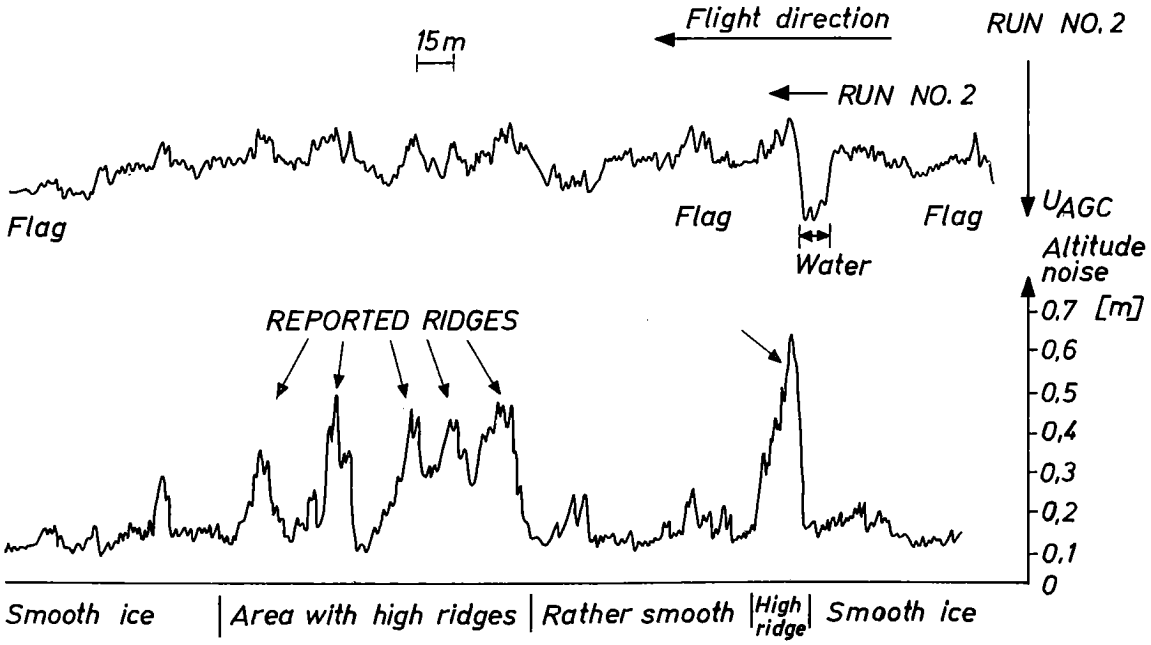

fluctuating noise level while the smooth ice reduces the altitude noise still more. The altitude noise varied between 0,45—0,6 m at the passage of the highest ice-ridges, which should be compared with their heights 1,6—1,9 m. The measured value of the altitude noise is thus typically 30% of the physical height of the ridge, which agrees well with the theoretical predictions according to Figure 2.2.

At the first run over the test area the helicopter passed over a small area of open water just in front of the highest ridge. As shown by Figure 5.3, an obvious increase in reflectance is shown by the AGC-signal at the passage over the water. Also the noise level is reduced, which indicates that the contribution from the ice-roughness in the side-lobes was negligible.

Figure 5.3: *The altitude noise and AGC-signal at a passage over the highest ridge in the area. (Expanded scale compared to Figures 5.1—5.2).*

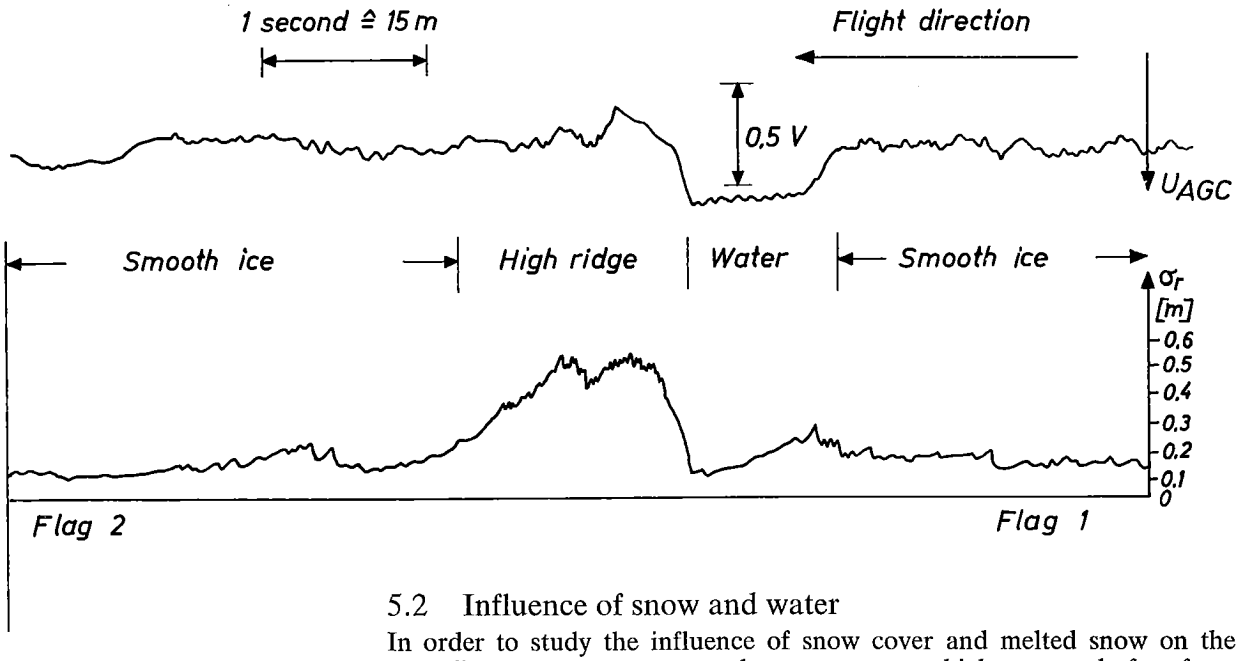

5.2 Influence of snow and water

In order to study the influence of snow cover and melted snow on the recordings, two runs were made over an area which was made free from snow. Half the area was flooded with water, and in the other part the ice-surface was only moisty. At the two ends of the area, there were compressed snow banks. The snow banks were generated by the vehicle, which cleared the ice of snow.

Figure 5.4 shows the altitude noise and the AGC-signal obtained at the first run. A very similar recording was obtained at the second run. As shown by the figure, the altitude noise is increased above the areas of snow banks but it is not so influenced by the water on the ice.

Figure 5.4: *Altitude noise and AGC-signal at a passage over a snow free area.*

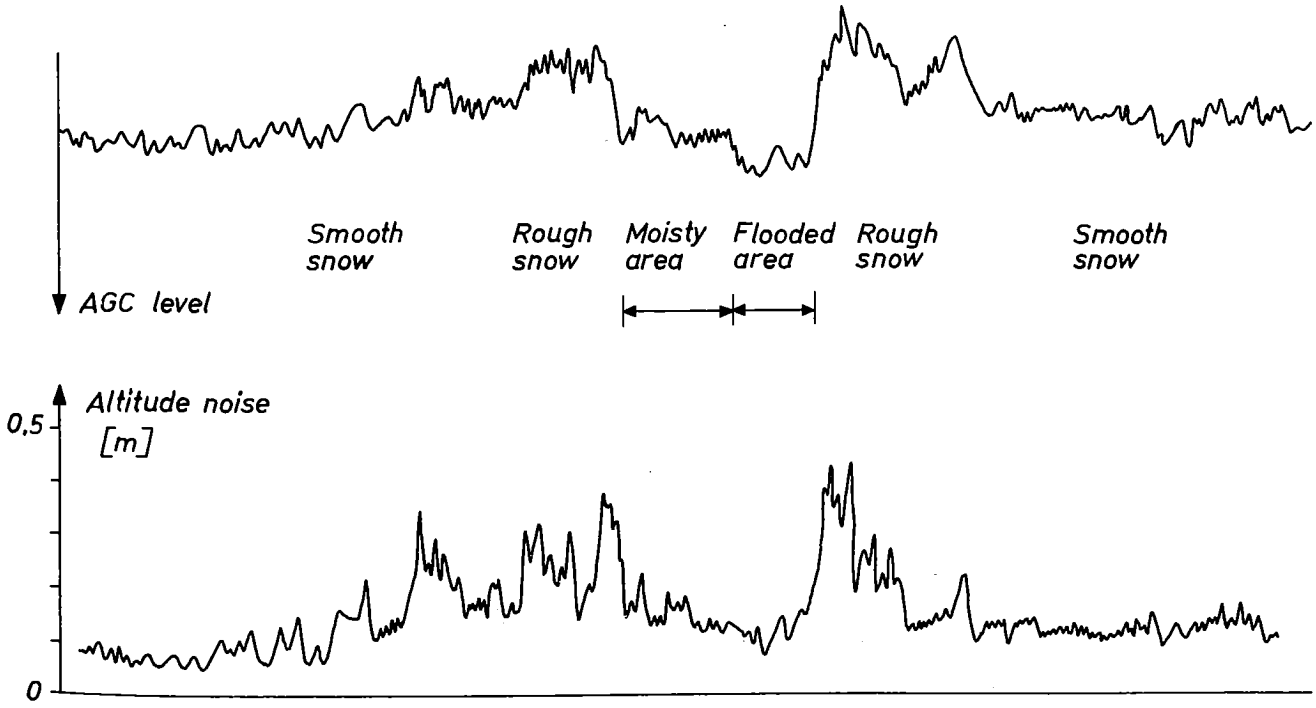

The AGC-signal indicates that the area, which is not covered by snow, has a significantly higher reflectance than the snow-covered ice. The flooded ice area has a somewhat higher reflectance than the moisty ice. The lowest reflectivity is obtained in the area of snow banks.

The experimental results agree well with the theory, taking into account the differences in dielectric constants between water, ice and snow. By the use of Fresnel's formula of the reflection coefficient at perpendicular incidence, the reflectivity of the different boundaries have been calculated in Figure 5.5.

Figure 5.5: *Typical values of the reflectivity of sea-ice, open water and snow-covered ice.*

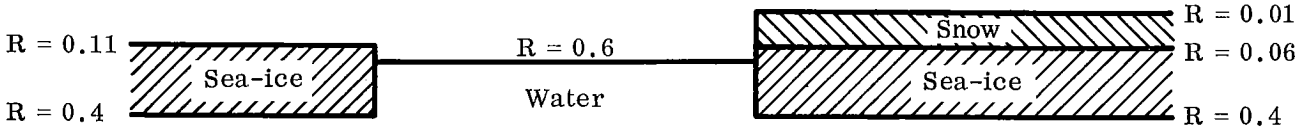

The reflectivity values of Figure 5.5 are only typical. An increased reflectivity from the ice is obtained at air temperatures above zero due to the increased content of liquid water. For lower temperatures (—10°C) the reflectivity of the ice is reduced as a consequence of the reduced dielectric constant. The reflectivity of the snow can also vary depending on the temperature and density of the snow cover. Hence, a 5—10 dB higher signal level can be expected from open water than from a sea-ice surface. If the ice is covered by snow the reflectivity is reduced still more.

When the ice is covered by a layer of water an increased reflectivity is obtained. As the penetration depth of water at 5 GHz is only about 3 mm, a relatively thin water layer effectively masks the signals from the underlying ice and gives the water covered ice-area the same reflectivity as open water.

5.3 Runs over thin ice

During the preliminary tests off Örnsköldsvik March 10, repeated runs were made above limited areas of smooth ice, not covered by snow and probably rather thin. The results showed a very low noise level above the smooth ice. Over the surrounding seasurface, which had a wave height of about 0,2—0,3 m, a significant increase in noise level was obtained. Both results agree with the theory.

In March 15, two runs were also made over an area with very thin ice, only about 0,03 m thick with roughnesses of the order of 0,01 m. At both runs, an increased noise level was obtained over the area of thin ice. There were no significant changes in the AGC-level. The reason for the increased noise level is not quite clear. Further studies on this problem are required.

5.4 Ice/water passages

Several passages from ice/water were made during the test period. Figure 5.6 shows the altitude noise at a passage from a rough water surface (wave-height 0,2—0,3 m) in over smooth and probably thin ice. As shown by the Figure, the noise level over the ice is reduced compared to the noise above the rough water surface.

Figure 5.6: *Passage over a water/ice boundary. The ice was smooth and free from snow. The wave-height of the water was 0,2—0,3 m.*

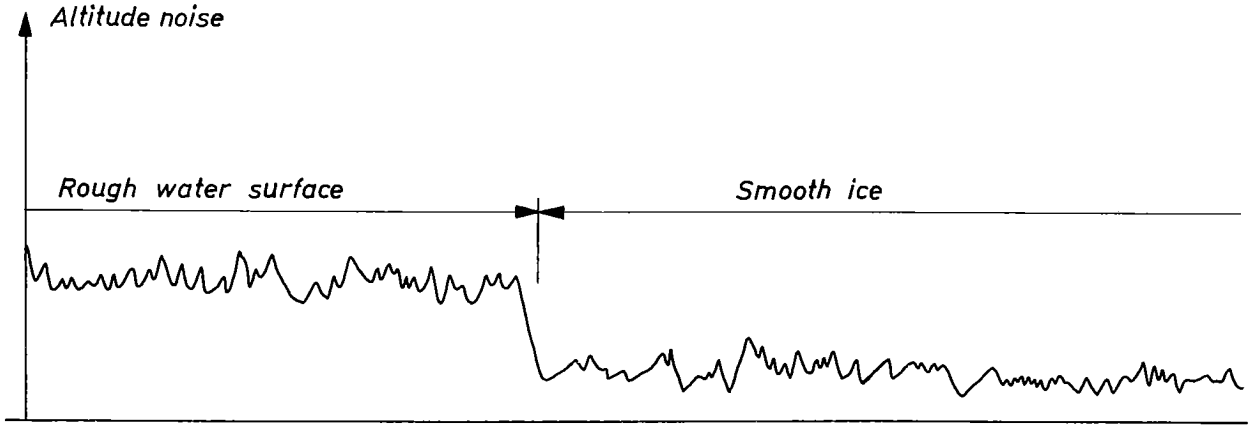

Figure 5.7 shows another recording obtained at a passage over a limited water area with only small waves. In that case, the altitude noise decreases over the water. The water has also a significantly higher reflectance than the ice (U_{AGC}). A similar results was obtained at the runs over the area of ice-ridges (Figure 5.3).

Figure 5.7: *Passage above an almost calm water area surrounded by sea-ice. From Luleå→TOR.*

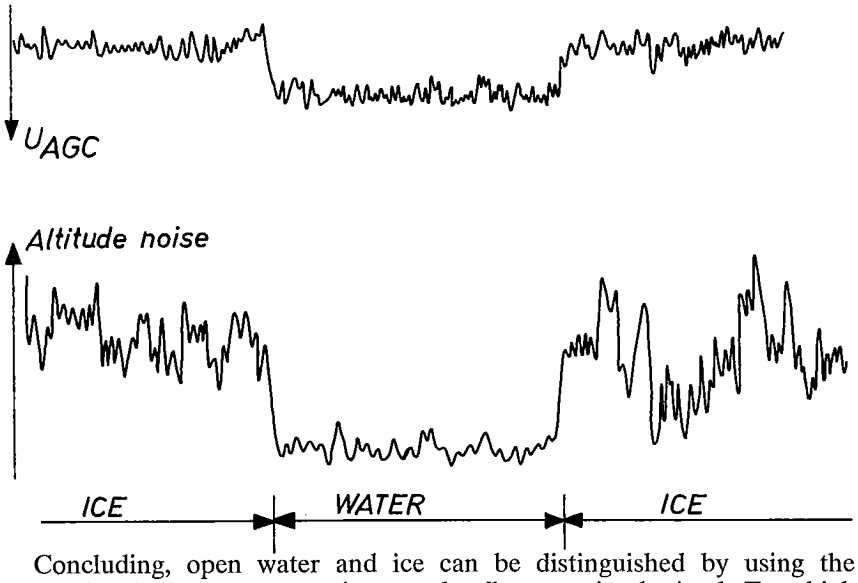

Concluding, open water and ice can be distinguished by using the AGC-signal. Over water an increased reflectance is obtained. For thick ice the change of the reflectance is typically 6 dB. The change of the altitude noise is depending on the roughness of the sea-surface and the ice. Also the ice-thickness has an influence. A smooth water surface (weak wind or a limited area of water) gives a low altitude noise which is similar to the results above thin smooth ice. A rough sea-surface like rough sea-ice, or thick ice increases the altitude noise of the output signal.

Figure 5.8: *Ice thickness measurements in the 1x1 km area.*

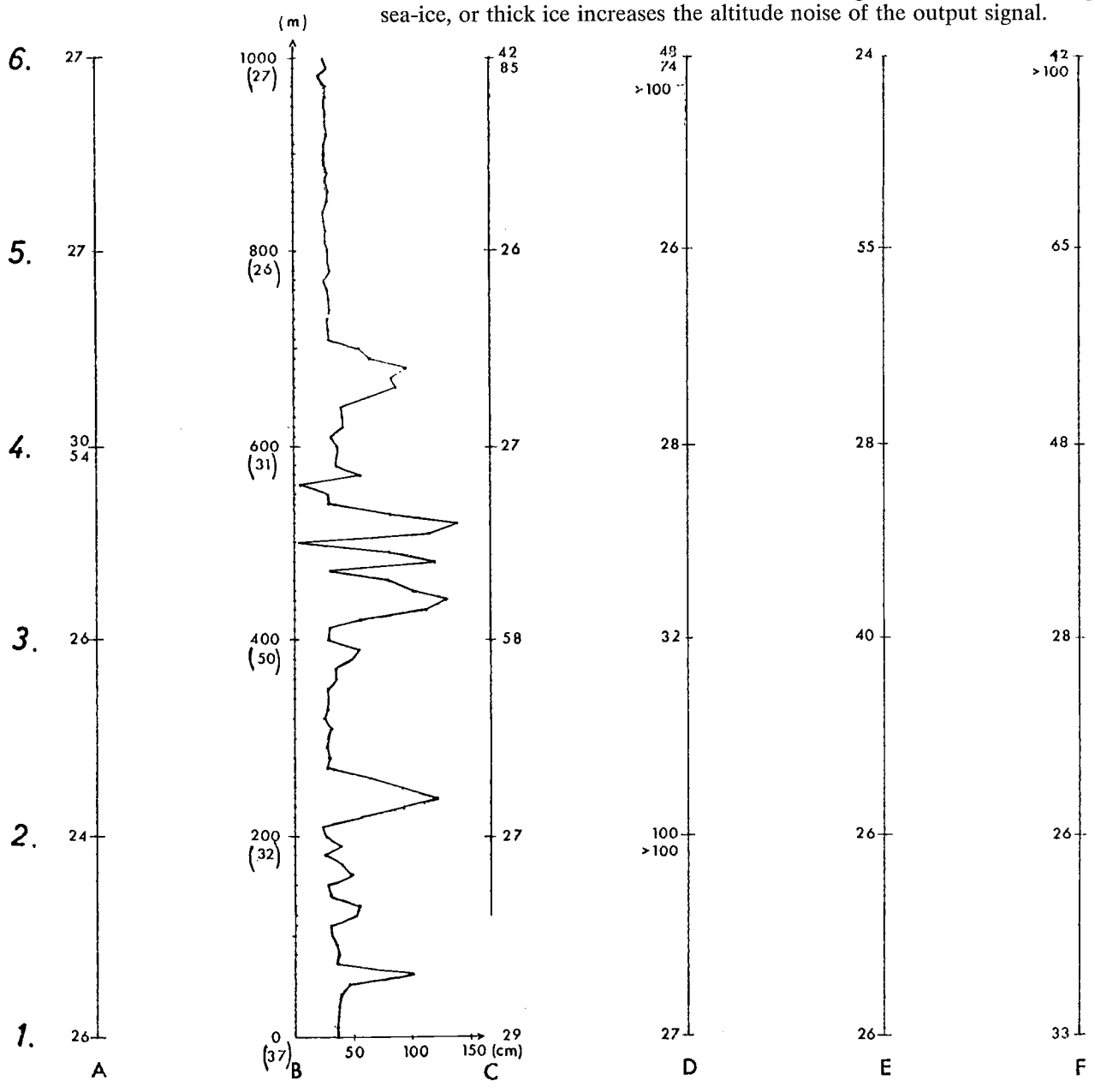

5.5 Recordings from the 1x1 km area

Runs along the different lines in the 1x1 km area were carried out on March 14. The obtained recordings of the altitude noise are shown in Figures 5.9—5.16. Figure 5.8 shows measured ice thickness at different points along the lines. In most cases, the thickness values are too few to give a detailed description of the ice thickness-fluctuations in the area. The ice-thickness in an area of compressed ice can vary strongly between two points, which are separated only a few meters. In particular there were strong variations along the B-line. Available information on the attenuation of the ice versus temperature indicates that the weather was too mild to permit ice-thickness measurements. Instead the large-scale surface roughness is expected to be the dominating parameter. A comparison between the available data of the ice surface roughness in the area and the recorded altitude noise, also shows an obvious correlation. In no case, the ice roughnesses were as high as the ridges recorded in Figures 5.1—5.3 (chapter 5.1). The results indicate that the altimetry information can be used to divide the mapped area into different roughness classes by using the fluctuations of the altitude noise level. Smooth ice gives a more constant and low noise level than is obtained over areas of rough ice. In case of ice ridges, a significant increase of the noise level is obtained at the passage.

Repeated runs were made along the B-line. Figures 5.10 and 5.11 show repeated runs at an altitude of 4 m. A good correlation between the recorded signals was obtained. The run at an altitude of 10 m (Figure 5.12) shows an increased noise level compared to the recordings from lower altitudes. This effect was expected as the slanting ranges to the reflectors within the antenna lobe increase the range spread at higher altitudes [3]—[4].

Theoretically, the range spread, introduced by the slanting ranges is about 0,3 m (rms) at 10 m altitude but only 0,1 m at 4 m with the existing antenna lobe (lobewidth 30 degrees). The slanting range effect, which degrades the accuracy at measurements of the surface roughness, can be reduced to a negligible level by reducing the lobewidth of the antenna. With a lobe width of 10 degrees, which corresponds to an antenna diameter of 0,5 m, the operative altitude can be increased to 30 m. For detection of large surface roughnesses like high ice ridges, a still higher altitude is permitted.

An analysis of the AGC-signal shows that this signal is usually reduced at a passage over a high ridge or areas of compressed ice. An example is shown in Figure 5.16. This effect is probably due to the fact that an ice ridge, consisting of ice floes with different orientations, reflects the incident radiation in a wider angular sector than a smooth ice surface. As a result, a smaller part of the reflected power is picked up by the receiver antenna above the rough ice surface.

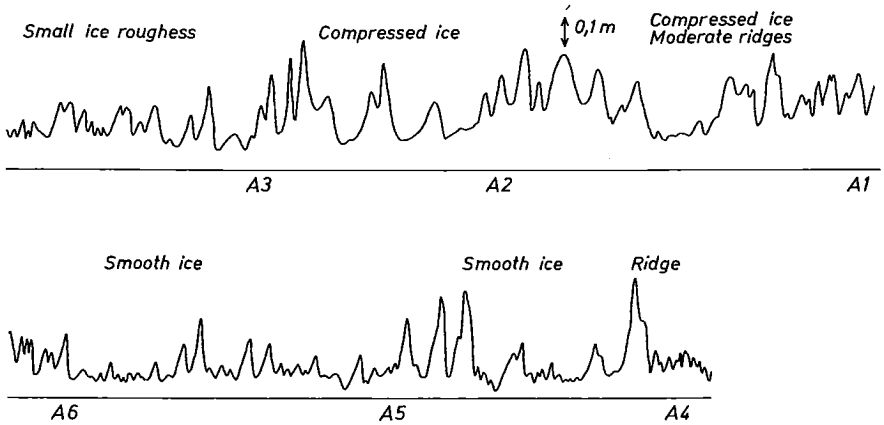

Figure 5.9: *Mean deviation of the altitude noise along the A-line in the 1x1 km area. Altitude: 4 m. Velocity: 30 knots.*

Figure 5.10: *Noise level along the B-line (first run). Altitude: 4 m. Velocity: 30 knots.*

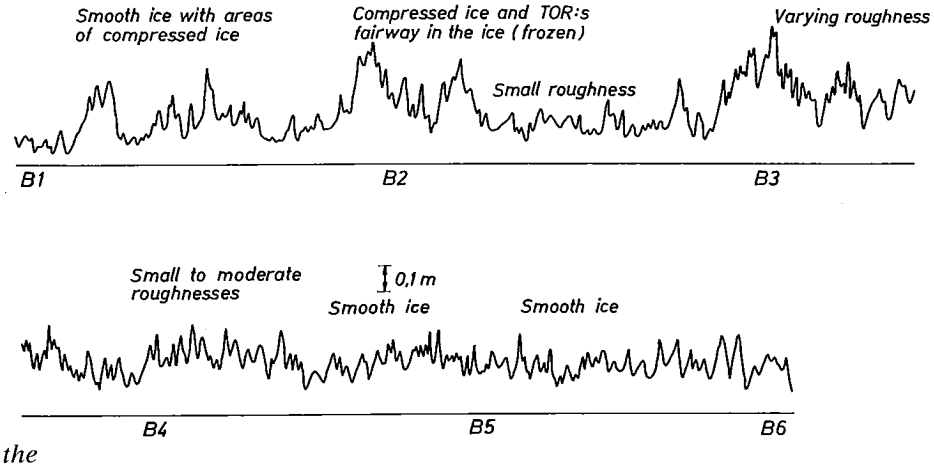

Figure 5.11: *Noise level along the B-line (second run). Altitude: 4 m. Velocity: 30 knots.*

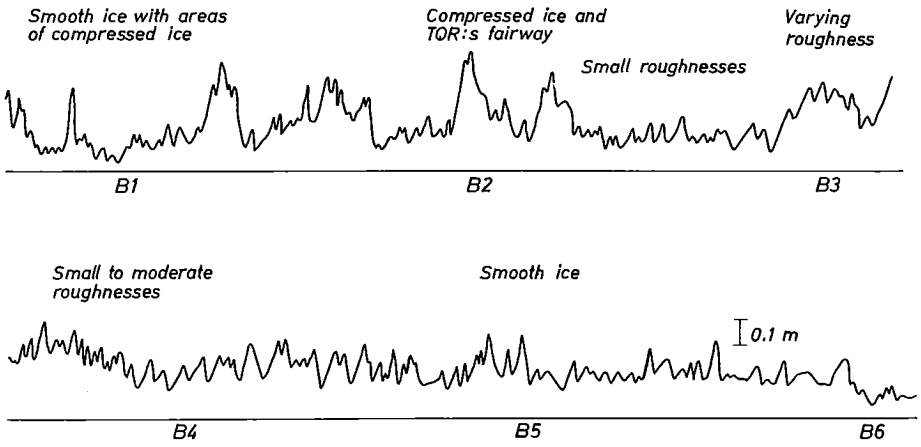

Figure 5.12: *Noise level along the B-line at a higher altitude: 10 m.*

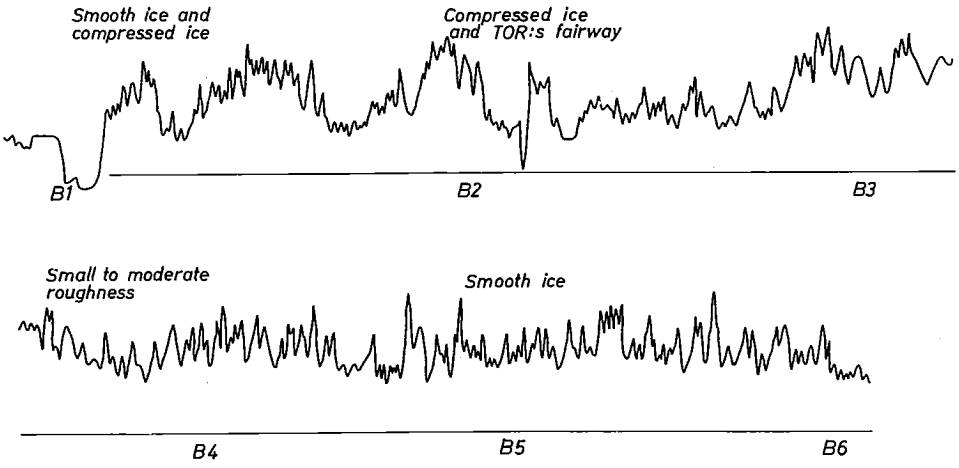

Figure 5.13: *Altitude noise along the D-line. Altitude: 4 m.*

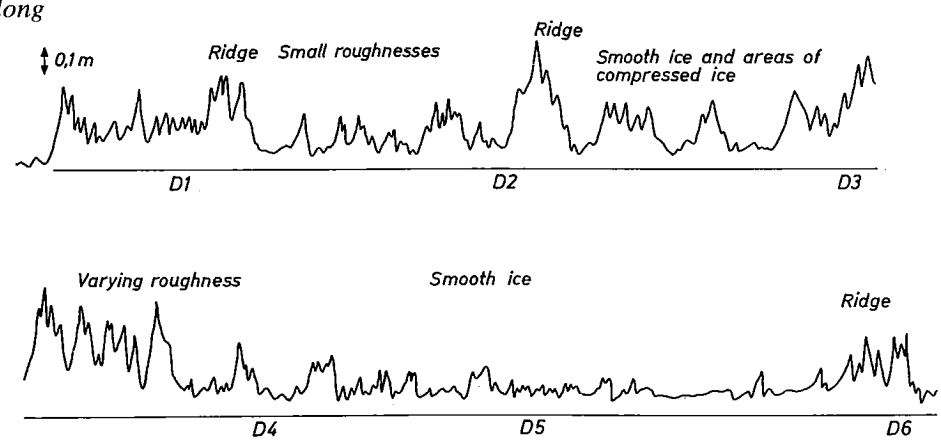

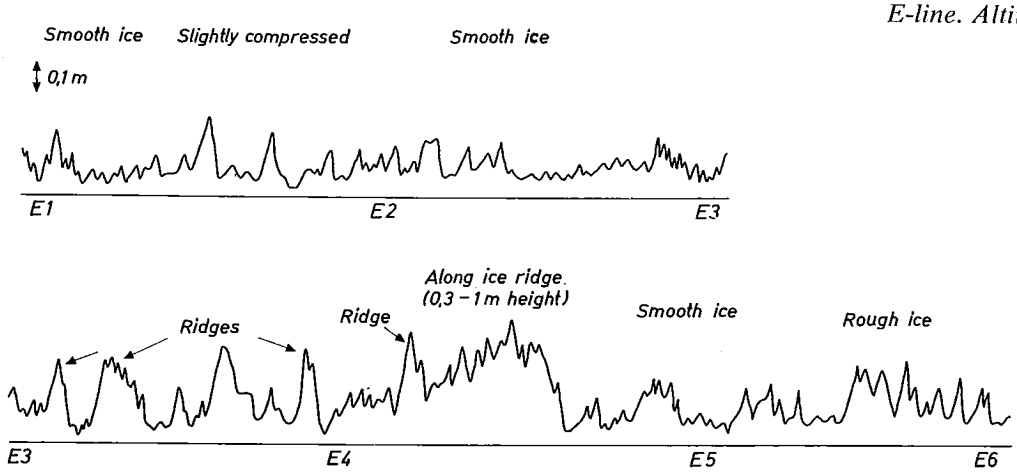

Figure 5.14: *Noise level along the E-line. Altitude: 4 m.*

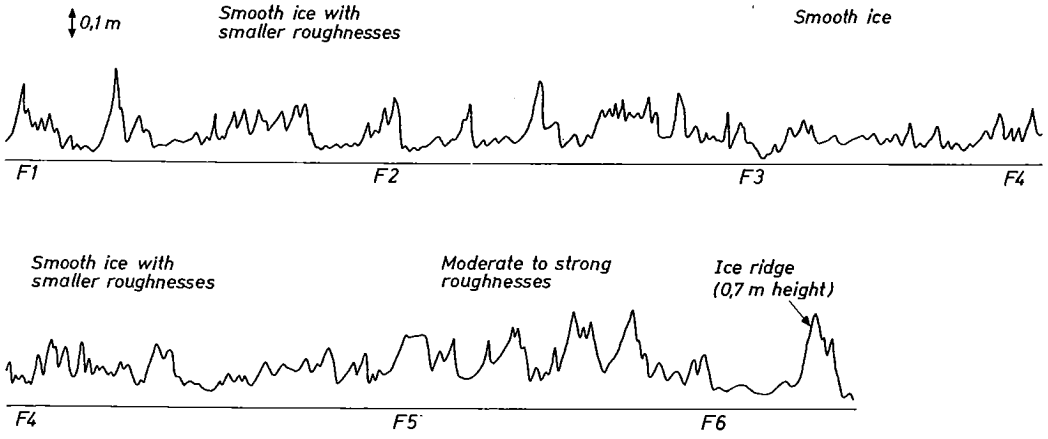

Figure 5.15: *Noise level along the F-line. Altitude 4 m.*

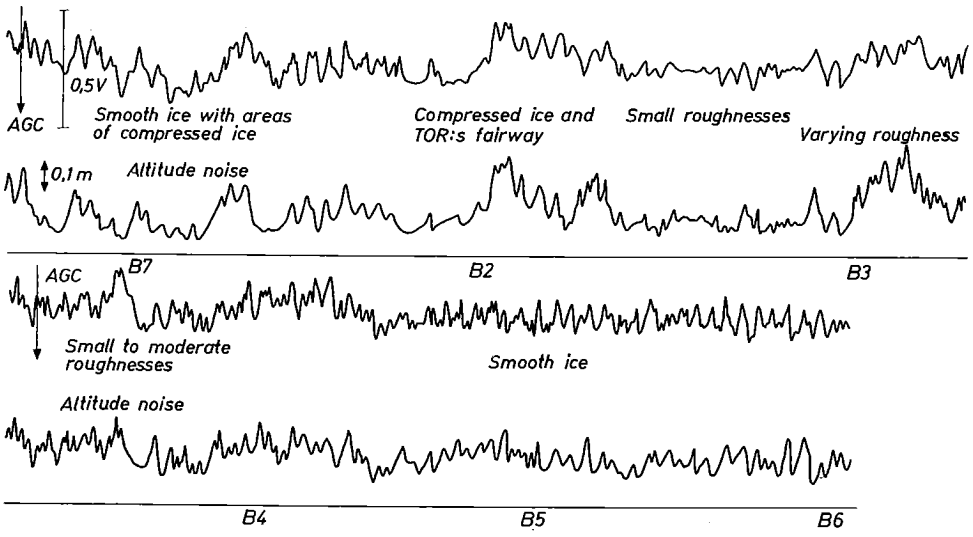

Figure 5.16: *Noise level and AGC-signal along the B-line.*

5.6 Spectral characteristics

The time fluctuations of a stationary noise signal can be characterized in statistical terms by its Wiener spectrum. If the time-fluctuations are rapid, most power is found at higher frequencies while slow variations give a contribution only at low frequencies. In order to investigate whether there are any spectral differences between the altimetry signals above different kinds of ground surfaces, limited parts of the recorded signals were analysed spectrally. Some representative results are found in Figures 5.17—5.18. As shown by the power spectrum of the AGC-signal (Figure 5.17), a rough water surface generates a morewideband AGC-signal than smooth ice. Similar results were obtained at the analysis of the altitude output signal. As shown by Figure 5.18, ice-areas with large surface roughnesses give a more wide-band signal than smoother ice-areas. Also the power content is significantly higher for the rough ice-surface. Generally, the bandwidth of the altitude noise is somewhat higher than the bandwidth of the AGC-signal. This difference is theoretically explained by the fact that the unsmoothed altitude output signal has passed a ratioformer, which increases the bandwidth [3].

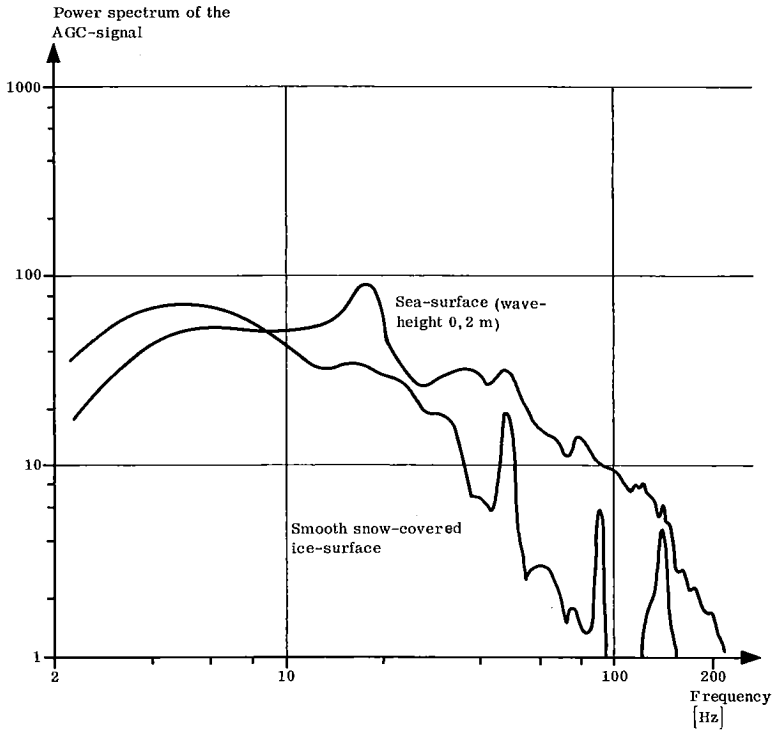

Figure 5.17: *Power spectrum of the AGC-signal obtained from flights above a rough sea-surface and a smooth ice area covered with snow.*

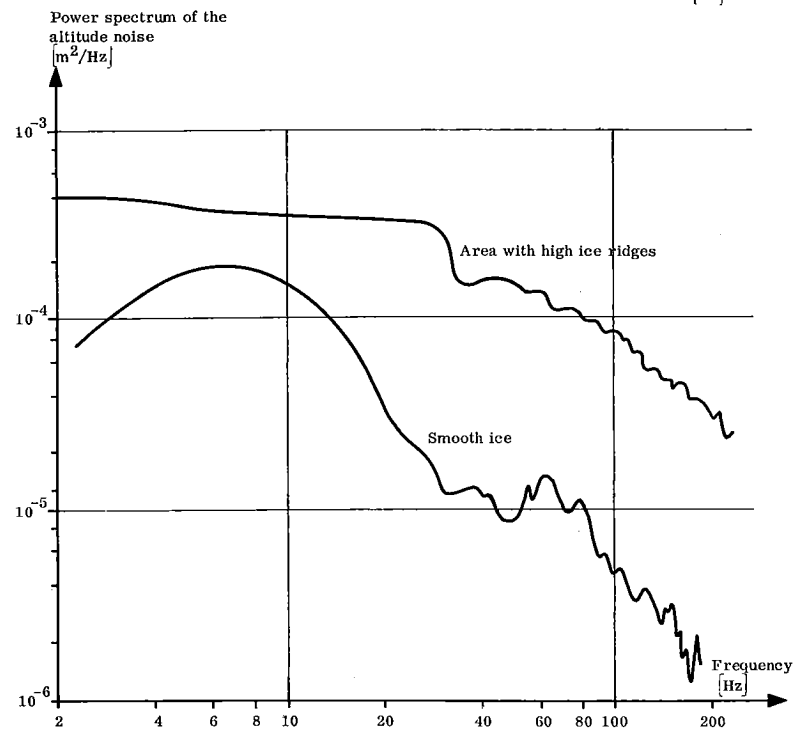

Figure 5.18: *Power spectrum of the altitude noise for flights above smooth ice and an area with high ice ridges.*

The obtained difference in bandwidths between signals received from a rough surface and a smooth one also agrees with the theory. Reflections close to the nadir direction give a lower doppler shift than is obtained in a more slanting direction when the velocity vector is parallel to the surface. As the reflected power from a smooth surface is concentrated to the nadir direction, a much smaller bandwidth is obtained than over a rough surface, from which reflections are also generated at oblique directions.

Concluding, the spectral analysis shows that the spectral properties of the altimetry signals can be useful to characterize the surface roughnesses. The bandwidth gives information about the average slope of the roughnesses and the total power content of the spectrum, which determines the mean noise variance, is a measure of the average surface roughness. If a scatterometer mode is included in the altimeter equipment, the similar type of information can be extracted as from a spectral analysis.

6. Conclusions and Recommendations

From the experimental results, the following preliminary conclusions can be drawn:

- ☐ the envelope-detected altitude noise seems to be a useful indicator of ice-ridges and large-scale surface roughnesses. The mean deviation of the noise component is correlated to the height of the roughnesses above the surrounding surface. There is a good agreement between theoretical models, describing the altitude noise from a rough ground surface and the experimental results concerning ice-ridges.
- ☐ ice with small-scale roughnesses can be distinguished from smooth ice as the roughnesses increase the bandwidth of the altitude signal. In case of a smooth ice surface, reflected energy is received only from surface elements close to the nadir direction, giving a smaller signal bandwidth.
- ☐ areas with open water can be separated from ice-covered areas by using the AGC-signal, which is a measure of the reflectance of the surface.
- ☐ snow-covered ice has a still lower reflectivity than noncovered ice.
- ☐ a thin water-layer on the ice gives an increased reflectivity which is close to the reflectivity of open water.

Thick and large ice ridges are time-consuming to cross even for an ice-breaker. Normal ice, even if it is relatively thick, does not cause any trouble for modern ice-breakers, however. Consequently, a radar altimeter installed on the helicopter of the ice-breaker can be used to localize large ice ridges. The instrument can also differentiate open water from ice and possibly measure the ice thickness. Contrary to laser profilers the radar altimeter can be used even at foggy weather and when the ice is covered by snow. Bad weather sometimes prevents visual ice surveys for weeks. Contrary to visual surveys, radar altimetry is not limited to day time.

A disadvantage with radar altimetry compared to imaging radars, is that the ice-situation is only recorded along the flight path of the helicopter, or the aircraft. However, the altimetry equipment can generate more quantitative data about the ice than can be obtained from a radar image. It might therefore be used by helicopters on ice-breakers in order to more carefully investigate a preliminary route, which has been selected on the basis of a radar image. The combined use of radar altimetry and microwave radiometry may also be a potential combination in the future. The microwave radiometer with a scanning or multi-lobe antenna can generate an image over the mapped area. However, its output signal seems to be more sensitive to the attenuation and the reflection properties of the sea-ice, which are varying due to snow-cover, moisture, air temperature [5]. The microwave radiometer is also less sensitive to ice ridges than the radar altimeter and gives no quantitative information of the ridge height.

The radar altimeter used at the experiment can be made more adapted for ice measurements after some modifications. A noise level detector should be implemented into the equipment for real-time operation. By increasing the size of the antennas, the operative altitude of the helicopter can be increased to at least 20—30 m. The implementation of a scatterometer mode would also make more information available.

The ice experiment of 1975 was carried out during a short period with milder weather than is normal during the winter. The air temperature influences to a great extent the content of free water on the ice-surface, in the snow and within the sea-ice. Quite different transmission and re-

flection properties of the snow and the ice can therefore be expected when the air temperature is decreased to less than —10°C [6]. Also the structure and porosity of the ice are varying over the ice period. Therefore, it is recommended that repeated field measurements are carried out during the winter 75/76. At these experiments, the effect of ice-thickness, snow depth and the influence of air temperature, ice-temperature should be studied. Theoretically, both the altitude noise and the AGC-signal have the capability to give some information about the ice-thickness, when the temperature of the ice is not too high (a semi-transparent ice layer is required). The experiments might be carried out from one of the helicopters, which are used by the ice-breakers and are not dependent on whether other sensors are used simultaneously. Some ground truth measurements on the ice along the flight paths are required, however. The tests should be limited to rather small well-defined areas of different types of ice, which are studied in very detail.

References

1. Blomquist Å, Pilo C & Thompson T: Sea Ice -75: Programme. Winter Navigation Research Board, Report No 16:1. Stockholm, Sweden, 1976.
2. Axelsson S: Programme for Sea-Ice Mapping by Radar Altimetry — March 1975.
   Saab-Scania report RL-0-3 B293, February 1975.
3. Axelsson S: Some characteristics of an amplitude or phase measuring CW-radar altimeter operating above a rough scattering ground surface. Saab Technical Notes, TN70, Linköping 1974.
4. Axelsson S: Some characteristics of frequency measuring FMCW radar altimeters operating above a rough ground surface. Report TR-157 Division of Applied Electronics, the Royal Institute of Technology, Stockholm 1975.
5. Axelsson S: Mapping of Sea-Ice by Radar Altimetry. Preliminary Study.
   Saab-Scania report RL-0-3 B275, December 1974.
6. Hallikainen M: Analysis of dielectric properties and noise temperature of sea ice for microwave remote sensing applications. Proc. 1973 European Microwave Conference, Brussels University, vol.2C.15.3.
7. Axelsson S: Amplitude and frequency measuring FMCW altimetry above a rough semi-transparent surface layer.
   Saab-Scania report RL-0-3 R32, August 1975.
8. Prof. M. Tiuri, Radio Laboratory, Helsinki University of Technology, private Communication.
9. Tiuri M, Hallikainen M, Kaski K: Experiments on Remote Sensing of sea ice using microwave radiometer. Radio Laboratory, Helsinki University of Technology, Report S67, 1974.

SWEDISH/FINNISH WINTER NAVIGATION RESEARCH BOARD

REPORTS

No. Titel

1. HAVSISKONFERENS. Protokoll (1972).
2. VINTERSJÖFART I BOTTENHAVET — Erfarenheter av SCA:s distributionssystem — L. Sjöstedt och S. Hammarsten (1972).
3. ISSKADOR PÅ FARTYG I ÖSTERSJÖN, BOTTENHAVET OCH BOTTENVIKEN. — Statistisk analys av skadefrekvenser — L. Sjöstedt och S. Hammarsten (1973).
4. PROPELLERPROBLEM. Propellerverkningsgradens beroende av bladutformningen. H.P. Loid (1973).
5. FARTYGS FRAMDRIVNINGSMOTSTÅND I IS. E. Enkvist (1974).
6. VINTERSJÖFART MED STORA FARTYG I BOTTENVIKEN. (1974).
7. VINTERSJÖFART I BOTTENVIKEN. Symposium Luleå (1974).
8. HAVSISUNDERSÖKNINGEN I BOTTENVIKEN VINTERN 1974. A. Omstedt, T. Thompson och I. Udin (1974).
9. KARTERING AV YTVATTENTEMPERATUREN I VATTNEN RUNT SVERIGE. J-E. Lundqvist, A. Omstedt och I. Udin (1974).
10. EXPERIMENTS ON REMOTE SENSING OF SEA ICE USING A MICROWAVE RADIOMETER. M. Tiuri, M. Hallikainen and K. Kaski (1974).
11. BOTTENVIKENS STÅLFYRAR — HÅLLFASTHETSANALYS OCH FÖRBÄTTRINGSFÖRSLAG. M. Määttänen (1974).
12. FORMATION AND STRUCTURE OF ICE RIDGES IN THE BALTIC. E. Palosuo (1975).
13. CALCULATION OF ICE DRIFT IN THE BOTHNIAN BAY AND THE QUARK. A. Valli and M. Leppäranta (1975).
14. A NARROW BEAM SONAR TO MEASURE THE SUBMARINE PROFILE OF AN ICE RIDGE. E. Palosuo, T. Pousi and M. Luukkala (1976).
15. THE AVERAGE SURFACE TEMPERATURE IN THE AUTUMN AND THE EARLY WINTER ON THE GULF OF BOTHNIA, THE NORTHERN BALTIC SEA AND THE GULF OF FINLAND (1966—1974). H. Grönvall and E. Palosuo (1976).

16:1 SEA ICE -75. Programme. Å. Blomquist, C. Pilo and T. Thompson (1975).

16:2 SEA ICE -75. Ground truth report. I. Udin (1976).

16:3 SEA ICE -75. Ice detection by SLAR. R.H.J. Morra and G.P. de Loor (1976).

16:4 SEA ICE -75. Analysis of SLAR data. S. Parashar (1976).

16:5 SEA ICE -75. FLAR, ODAR, ship's radar. J. Nilsson, T. Hagman and Y. Nilsson (1976).

16:6 SEA ICE -75. IR-scanner results. E. Fagerlund and G. Lundholm (1976).

16:7 SEA ICE -75. Radaraltimeter results. S. Axelsson (1976).

16:8 SEA ICE -75. Dynamical report. I. Udin and A. Omstedt (1976).

16:9 SEA ICE -75. Summary report. Å. Blomquist, C. Pilo and T. Thompson (1976).